In fact, Wink and co-workers[23] have shown that in other systems this is a useful method for directing regio- and stereospecific electrophilic attack on a diene ligand.

Our attempts to isolate the products resulting from the reaction between a molybdenum *trans*-diene complex and HBF_4 have been unsuccessful and very frustrating. There appears to be more than one organometallic product of the reaction, as evidenced by a very broad (100 cm^{-1}) ν_{NO} band in the IR spectrum of the reaction mixture and several resonances in the Cp region of the proton NMR spectrum of the reaction residue. Furthermore, all attempts to separate and purify the mixture lead to decomposition of all nitrosyl-containing species. An interesting addendum to these observations is that, whatever the organometallic species are in the final reaction mixture, they are stable with respect to attack by H^- (e.g. $NaBH_4$ and Red-Al).

In summary, it appears that more study of this latter area is needed in order to define properly the limits of the reactions of the *trans*-diene complexes with electrophiles. For instance, our observations to date do not rule out that oxidation of the organometallic reactants may well also be occurring upon their treatment with H^+. Nevertheless, it is also clear from the studies described in this paper that nucleophilic attack on the *trans*-diene complexes does not lead to concomitant reduction. Hence, these reactivity patterns are fully in accord with the molecular orbital description of the bonding of these interesting organometallic complexes.[5]

Acknowledgment. We are grateful to the Natural Sciences and Engineering Research Council of Canada for support of this work in the form of grants to P.L. and F.W.B.E.

Supplementary Material Available: Tables of positional and thermal parameters for the hydrogen atoms and anisotropic thermal parameters for the non-hydrogen atoms for each of the complexes 1A and 2 and bond lengths and bond angles involving the hydrogen atoms of 2 (10 pages); listings of the observed and calculated structure factors for both complexes (36 pages). Ordering information is given on any current masthead page.

---

[23] Wink, D. J.; Wang, N. F.; Springer, J. P. *Organometallics* 1989, *8*, 259.

Oxymethylation of Alkyliron Complex $CpFe(CO)_2$–R with Hydrostannane and -silane, Leading to R–CH_2OH Derivatives: Related Reactions of CpFe(CO)(L)–R and CpFe(CO)(L)–C(O)R Type Organoiron Complexes and the Molecular Structure of *trans*-$CpFe(H)(CO)(SnPh_3)_2$

Munetaka Akita,* Tomoharu Oku, Masako Tanaka, and Yoshihiko Moro-oka*

Research Laboratory of Resources Utilization, Tokyo Institute of Technology, 4259 Nagatsuta, Midori-ku, Yokohama 227, Japan

Received February 8, 1991

Thermal reaction of an alkyliron complex $CpFe(CO)_2$–R (1) (R = CH_2CH_2Ph) and acyliron complexes, $CpFe(CO)_2$–C(O)R (3) and $CpFe(CO)(PPh_3)$–C(O)R (4) with 3 equiv of $HMMe_3$ (M = Sn, Si) affords the oxymethylated product R–CH_2OX (5) in excellent yields accompanied by the formation of CpFe(H)-(L)$(MMe_3)_2$ (**9a** L = CO, M = Sn; **10a** L = CO, M = Si; **11** L = PPh_3, M = Sn). The reaction of a phosphine-substituted alkyliron complex $CpFe(CO)(PPh_3)$–R (2) under similar reaction conditions gives R–H (7). On the other hand, irradiation of the organoiron complexes 1–4 in the presence of $HMMe_3$ produces 7 as a major product with the exception of 3 + $HSnMe_3$ where R–CHO (6) is obtained. The thermal reaction is found to consist of two consecutive reactions, i.e., formation of 6 and reduction of 6 to 5. When $HSnMe_3$ is used as a limiting substrate ($HSnMe_3/1 \le 2$), R–CHO is actually formed in good yield. The second step is proved to be catalyzed by various iron complexes such as **9a**, Fp–Me, Fp–C(O)Me, and Fp_2. The relationship among 1–4 and the coordinatively unsaturated species is also discussed. The molecular structure of *trans*-$CpFe(H)(CO)SnPh_3)_2$ (**9c**) obtained by the thermal reaction of 1 with $HSnPh_3$ has been determined by X-ray diffraction study. The unit cell contains two crystallography independent molecules with the essentially same geometry. The structure is described as a four-legged piano stool structure with the two $SnPh_3$ groups occupying the mutually trans basal positions. The contribution of the η^2-coordination mode of the H–Sn bond may be negligible on the basis of the molecular structure as well as the small ^2J(H–Fe–Sn) values. Crystal data for **9c**: space group $P\bar{1}$, $a = 16.248$ (7) Å, $b = 19.646$ (6) Å, $c = 11.443$ (5) Å, $\alpha = 93.32$ (3)°, $\beta = 93.67$ (4)°, $\gamma = 97.09$ (3)°, $V = 3609$ (3) Å^3, $Z = 4$, $R = 0.0312$, $R_w = 0.0379$.

Introduction

Reductive cleavage of a transition metal–carbon bond plays an important role in the product-releasing step of a variety of catalytic reactions including hydrogenation and hydroformylation.[1] For example, in the former reaction oxidative addition of hydrogen to an alkylmetal species leads to the formation of a (dihydrido)(alkyl)metal species, which reductively eliminates the product, alkane.

On the other hand, it has been revealed that hydrosilane and -stannane exhibit reactivities similar to those of hydrogen with respect to oxidative addition to a low-valent metal center.[1,2] In addition to this feature, silicon and tin

---

[1] Collman, J. P.; Hegedus, L. S.; Norton, J. R.; Finke, R. G. *Principles and Applications of Organotransition Metal Chemistry*, 2nd ed.; University Science Book: Mill Valley, CA, 1987.

0276-7333/91/2310-3080$02.50/0

Table I. Reaction of Iron Complexes CpFe(CO)(L)–org 1–4 with 3 Equiv of $HMMe_3$ (M = Sn, Si)[a]

	complex					organic products[b]				organometallic products[c]				
entry		org	L	M	reacn conditions	**5**	**6**	**7**	**8**	**9a (10a)**	**11**	**12**	**13**	**14**
1	1	R	CO	Sn	90 °C, 3 h	94 (**5c**)	0	tr		89		0	0	0
2	1	R	CO	Si	90 °C, 9 h	98 (**5b**)	0	0	0	90		0	10	0[d]
3	2	R	PPh_3	Sn	100 °C, 6 h	tr (**5c**)	0	85		86	0	0	0	0
4	2	R	PPh_3	Si	120 °C, 6 h	11 (**5b**)	0	64	0	0	0	42 (**12d**)	20	15
5	3	C(O)–R	CO	Sn	120 °C, 7 h	96 (**5c**)	tr	0		tr		93 (**12a**)	0	0
6	3	C(O)–R	CO	Si	120 °C, 10 h	53 (**5b**)	tr	tr	14	0		28 (**12b**)	72	0
7	4	C(O)–R	PPh_3	Sn	120 °C, 6 h	91 (**5c**)	tr	tr		91[e]	0	7 (**12c**)[e]	0	0
8	4	C(O)–R	PPh	Si	100 °C, 18 h	81 (**5b**)	0	0	tr	0	0	37 (**12d**)[e]	tr[e]	31[e]
9	1	R	CO	Sn	*h*v, 7 h	0	0	86		95		0	0	0
10	1	R	CO	Si	*h*v, 12 h[f]	0	0	70	0	47		0	40	0
11	2	R	PPh	Sn	*h*v, 19 h	0	0	84		0	83	0	0	0
12	2	R	PPh_3	Si	*h*v, 18 h[f]	0	0	65	0	0	0	7 (**12d**)[e]	0	0
13	3	C(O)–R	CO	Sn	*h*v, 6 h	0	79	0		92		0	0	0
14	3	C(O)–R	CO	Si	*h*v, 15 h	22 (**5b**)	tr	28	39	24[e]		0	70	0
15	4	C(O)–R	PPh	Sn	*h*v, 24 h	tr (**5c**)	0	37		0	43[e]	8 (**12c**)[e]	0	0
16	4	C(O)–R	PPh_3	Si	*h*v, 18 h	8 (**5b**)	0	42	0	0	0	20 (**12d**)[e]	31[e]	0

[a] R: CH_2CH_2Ph. Scale: ca. 0.2 M in C_6D_6. Photochemical reactions were carried out at room temperature. Conversion: 100% except entries 15 and 16 (90% and 65% conversion, respectively). tr: <3%. See also ref 8. [b] Determined by means of GLC. **5**: $R–CH_2OX$. **6**: R–CHO. **7**: R–H. **8**: $PhCH_2CH{=}CHOSiMe_3$. [c] Determined by means of ^1H NMR spectroscopy unless otherwise stated. **9a**: CpFe(H)(CO)$(SnMe_3)_2$. **10a**: CpFe(H)(CO)$(SiMe_3)_2$. **11**: CpFe(H)$(PPh_3)(MMe_3)_2$. **12a**: $CpFe(CO)_2–SnMe_3$. **12b**: $CpFe(CO)_2–SiMe_3$. **12c**: $CpFe(CO)(PPh_3)–SnMe_3$. **12d**: $CpFe(CO)(PPh_3)–SiMe_3$. **13**: Fp_2. [d] $[CpFe(CO)]_4$ was formed in 10% yield. [e] Isolated yield. [f] Styrene was also formed in 17% (entry 10) and 12% (entry 12) yields.

possess high affinity toward an oxygen-containing functional group in an organic molecule. These features have been successfully applied to such catalytic reactions as hydrosilylation of organic carbonyl compounds[3] and the $Co_2(CO)_8$-catalyzed siloxymethylenation of oxiranes and alkenes.[4]

In previous papers we reported the Rh(I)-catalyzed hydrosilylation of various transition-metal acyl complexes giving partially reduced α-siloxyalkyl or fully reduced alkyl complexes.[5,6] During the course of our study we have found that alkyl- and acyliron complexes react with hydrostannane and -silane in the absence of the Rh(I) catalyst to give $R–CH_2OH$ derivatives. This reaction includes activation of the H–M bond in hydrostannane and -silane at an iron center and reductive cleavage of a metal–carbon bond. Herein we disclose the detailed results of the reaction of organoiron complexes with these reducing agents under thermal and photochemical conditions.[7] In addition, the molecular structure of CpFe(H)(CO)$(SnPh_3)_2$, one of the organometallic products, has been determined by an X-ray diffraction study.

Results and Discussion

Thermal Reaction of Organoiron Complexes $CpFe(CO)_2–R$ (1), $CpFe(CO)(PPh_3)–R$ (2), $CpFe(CO)_2–C(O)R$ (3), and $CpFe(CO)(PPh_3)–C(O)R$ (4) (R = CH_2CH_2Ph) with $HMMe_3$ (M = Sn, Si) Leading to $R–CH_2OH$ Derivatives. Phenethyl derivatives (R = CH_2CH_2Ph) of alkyliron complexes $CpFe(CO)_2–R$ (1) and $CpFe(CO)(PPh_3)–R$ (2) and acyliron complexes $CpFe(CO)_2–C(O)R$ (3) and $CpFe(CO)(PPh_3)–C(O)R$ (4) were chosen as substrates because of easy handling and analyses.

Table II. Thermal Reaction of 1 with 3 Equiv of HMR'_3

HMR'_3	reacn conditions	**5c**	**6**	**7**	**15**[a]	**9 or 10**
$HSnBu_3$	120 °C, 1 h	70	8	0	0	90 (**9b**)[b]
$HSnPh_3$	90 °C, 2 h	61	0	8	0	87 (**9c**)[b]
$HSiEt_3$	120 °C, 2 h	79[c]	0	tr	0	3 (**10b**)[d]
H_2SiEt_2	120 °C, 2 h	70[c]	0	tr	8	0
$HSiPh_3$	120 °C, 10 h	52[c]	0	tr	4	0
H_2SiPh_2	120 °C, 2 h	77[c]	0	0	5	83 (**10c**)[b]
H_3SiPh	120 °C, 2 h	54[c]	0	0	13	0

[a] **15**: $R–CH_3$. [b] NMR yields. [c] Yields were determined after treatment with methanolic KF solution. [d] Isolated yield.

Thermal reaction of the iron complexes 1–4 with 3 equiv of $HMMe_3$ (M = Sn, Si) was carried out in heated benzene in a sealed NMR tube or a closed Schlenk tube, and typical results are summarized in Table I[8] (entries 1–8). As a result, the oxymethylated product **5**[9,10] was formed in excellent yields from the dicarbonylalkyl complex 1 and the acyl complexes 3 and 4 (eq 1, entries 1, 2, and 5–8 of Table I). On the other hand, alkane, R–H (7), was obtained as

$$\left.\begin{array}{ll} CpFe(CO)_2–R & (1)\\ CpFe(CO)_2–C(O)R & (3)\\ CpFe(CO)(PPh_3)–C(O)R & (4)\end{array}\right\} + 3HMMe_3 \xrightarrow[\text{benzene}]{\Delta}$$

$$(R = CH_2CH_2Ph)$$

$$\begin{array}{ccc} R–CH_2OX & + & CpFe(H)(CO)(MMe_3)_2 \; + \\ \mathbf{5a}: X = SnMe_3 & & \mathbf{9a}: M = Sn \\ \mathbf{5b}: X = SiMe_3 & & \mathbf{10a}: M = Si \\ \mathbf{5c}: X = H & & \end{array}$$

$$\begin{array}{l} CpFe(CO)(L)(MMe_3) \qquad (1) \\ \mathbf{12a}: L = CO, M = Sn \\ \mathbf{12b}: L = CO, M = Si \\ \mathbf{12c}: L = PPh_3, M = Sn \\ \mathbf{12d}: L = PPh_3, M = Si \end{array}$$

---

(2) Mackay, K. M.; Nicholson, B. K. In *Comprehensive Organometallic Chemistry*; Wilkinson, G., Stone, F. G. A., Eds.; Pergamon Press: Oxford, U.K., 1982; Vol. 6, Chapter 43.

(3) Ojima, I.; Hirai, K. In *Asymmetric Synthesis*; Morrison, E. D., Ed.; Academic Press: New York, 1985; p 103.

(4) (a) Murai, S.; Sonoda, N. *Angew. Chem., Int. Ed. Engl.* **1979**, *18*, 393. (b) Murai, S.; Seki, Y. *J. Mol. Catal.* **1987**, *41*, 197. (c) Murai, T.; Yasui, E.; Kato, S.; Hatayama, Y.; Suzuki, S.; Yamasaki, Y.; Sonoda, N.; Kurosawa, H.; Kawasaki, Y.; Murai, S. *J. Am. Chem. Soc.* **1989**, *111*, 7938.

(5) (a) Akita, M.; Mitani, O.; Moro-oka, Y. *J. Chem. Soc., Chem. Commun.* **1989**, 527. (b) Akita, M.; Mitani, O.; Sayama, M.; Moro-oka, Y. *Organometallics* **1991**, *10*, 1394.

(6) (a) Crawford, E. J.; Hanna, P. K.; Cutler, A. R. *J. Am. Chem. Soc.* **1989**, *111*, 689. (b) Gregg, B. G.; Hanna, P. K.; Crawford, E. J.; Cutler, A. R. *J. Am. Chem. Soc.* **1991**, *113*, 384. (c) Hanna, P. K.; Gregg, B. G.; Cutler, A. R. *Organometallics* **1991**, *10*, 31.

(7) A preliminary communication of part of this study has already appeared: Akita, M.; Oku, T.; Moro-oka, Y. *J. Chem. Soc., Chem. Commun.* **1989**, 1790.

(8) In the preliminary communication[7] the organoiron product (**12a**) of entry 5 was incorrectly assigned as **9a**.

(9) Although, strictly speaking, the reaction of **3** and **4** is not "oxymethylation", we use this term for these substrates throughout this paper.

(10) **5a** was observed by NMR experiments but decomposed in a GLC column to give **5c**.

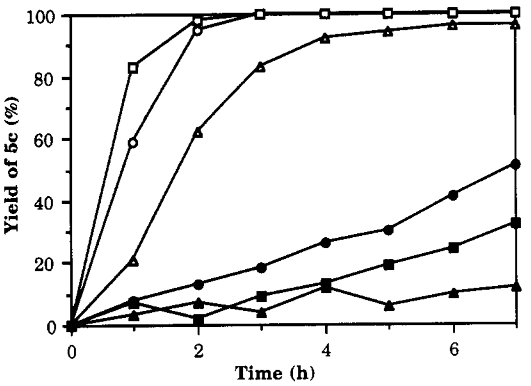

Figure 1. Catalytic hydrostannylation of $PhCH_2CH_2CHO$ (**7**) with $HSnMe_3$ in the presence of 10 mol % of iron complexes (in benzene-d_6 at 120 °C): (□) **13**; (○) **9a**; (△) Fp–Me; (●) Fp–C(O)Me; (■) **12a**; (▲) none.

a major organic product from the phosphine-substituted alkyl complex **2** (entries 3 and 4 of Table I) (eq 2). As

$$\mathbf{2} + 3HMMe_3 \xrightarrow[\text{benzene}]{\Delta} \text{R–H} + \mathbf{9a} \text{ or } \mathbf{12} \qquad (2)$$

to the organometallic products, the reaction with $HSnMe_3$ gave $CpFe(CO)(H)(SnMe_3)_2$ (**9a**) or $CpFe(CO)(L)(SnMe_3)$ [**12a** (L = CO), **12c** (L = PPh_3)] as a major product, and the reactions with $HSiMe_3$ gave a mixture of variable amounts of $CpFe(CO)(H)(SiMe_3)_2$ (**10a**), $CpFe(CO)(L)(SiMe_3)$ [**12b** (L = CO), **12d** (L = PPh_3)], Fp_2 (**13**), Cp_2Fe (**14**), and $[CpFe(CO)]_4$.[11]

On the ground of the reaction conditions, $HSnMe_3$ appeared to be more reactive than $HSiMe_3$. (For example, **1** reacted with $HSnMe_3$ even at 60 °C, but it took 12 h for completion of the reaction. See also entries 1 and 2 in Table I.) In addition, hydrostannanes and -silanes other than $HMMe_3$ were also effective for the present oxymethylation reaction, as shown in Table II.[12] Although **5c** was formed in satisfactory yields in every case, $HSnMe_3$ was the best reducing agent of the group 14 metal hydrides employed, and no apparent substituent effect was observed except that $H_nSiR'_{4-n}$ with larger n afforded R–CH_3 (**15**)[13] in slightly higher yield. The excess H_3SiPh was completely converted to H_2SiPh_2 after the reaction.[14]

Photochemical Reaction of Organoiron Complexes 1–4 with $HMMe_3$ (M = Si, Sn). Photochemical reaction of **1–4** resulted in completely different product distributions (eqs 3 and 4, entries 9–16 in Table I). Except entry 13 where R–CHO (**6**) was formed as the sole organic product in 79% yield (eq 4), the major organic product was R–H (**7**) (eq 3). In this case, too, the major organometallic product obtained by the reaction with $HSnMe_3$ was **9a** or **11**, and the reaction with $HSiMe_3$ afforded a mixture of variable amounts of **10a–14**.[11]

$$\mathbf{1, 2, 4} + 3HMMe_3 \xrightarrow[\text{benzene}]{h\nu} \text{R–H} + \mathbf{9–12} \qquad (3)$$

$$\mathbf{3} + 2HSnMe_3 \xrightarrow[\text{benzene}]{h\nu} \underset{\mathbf{6}}{\text{R–CHO}} + \mathbf{9a} \qquad (4)$$

Thermal Reaction Leading to R–CHO and Subsequent Reduction to R–CH_2OMMe_3. When the thermal oxymethylation of **1** with $HSnMe_3$ was monitored by ^1H NMR spectroscopy a small amount of R–CHO (**6**) was occasionally observed and finally converted to **5**. This result suggests that the oxymethylation of **1** (eq 7) may consist of two consecutive reactions, that is, formation of R–CHO **6** (eq 5) and reduction of **6** to **5** by HMR'_3 (eq 6). Actually, when less than 2 equiv of $HSnMe_3$ was used, R–CHO was formed in good yield together with the formation of a comparable amount of **9a** (eqs 8 and 9).

$$\underset{\mathbf{1}}{CpFe(CO)_2\text{–R}} + 2HMMe_3 \longrightarrow \underset{\mathbf{6}}{\text{R–CHO}} + \underset{\mathbf{9a,\,10a}}{CpFe(H)(CO)(MMe_3)_2} \qquad (5)$$

$$\underset{\mathbf{6}}{\text{R–CHO}} + HMMe_3 \xrightarrow{\text{cat.}} \underset{\mathbf{5}}{\text{R–}CH_2OMMe_3} \qquad (6)$$

$$\underset{\mathbf{1}}{CpFe(CO)_2\text{–R}} + 3HMMe_3 \longrightarrow \underset{\mathbf{5}}{\text{R–}CH_2OMMe_3} + \underset{\mathbf{9a,\,10a}}{CpFe(H)(CO)(MMe_3)_2} \qquad (7)$$

$$\mathbf{1} + HSnMe_3 \longrightarrow {}^1/_2\mathbf{6} + {}^1/_2\mathbf{9a} \qquad (8)$$

$$\begin{array}{lll} \text{70 °C, 2.5 h} & 90\% & 100\% \\ \text{90 °C, 0.5 h} & 80\% & 82\% \\ & \multicolumn{2}{c}{\text{(based on } HSnMe_3)} \end{array}$$

$$\mathbf{1} + 2HSnMe_3 \xrightarrow[\text{80 °C, 5 h}]{} \underset{71\%}{\mathbf{6}} + \underset{10\%}{\mathbf{5c}} + \underset{93\%}{\mathbf{9a}} \qquad (9)$$

(based on **1**)

The second step (eq 6) slowly proceeded in heated benzene without any additives, but the reaction was much slower than the total oxymethylation of **1** (eq 7). This result suggested that some iron species worked as a catalyst for eq 6. In fact, the addition of a catalytic amount (10 mol %) of a certain iron complex [Fp–alkyl and -acyl, **9a**, and Fp-$SnMe_3$ (**12a**)[15]] to the reaction mixture resulted in a marked acceleration of the reaction rate as shown in Figure 1 (eq 10). Even a simple dinuclear iron complex, Fp_2 (**13**),[16] showed a catalytic activity, and the order of the reaction rate was estimated as follows: **9a** ≅ **13** > Fp–Me > Fp–C(O)Me > **12a**. The iron complex recovered from the reaction mixture was **9a** (from Fp–Me, Fp–C(O)Me, and **9a**) and **12a** (from **12a** and **13**).

$$\underset{\mathbf{5}}{\text{Ph–}CH_2CH_2\text{–CHO}} + HSnMe_3 \xrightarrow[\substack{120\ °C \\ C_6D_6}]{\substack{\text{Fe complex} \\ \text{(10 mol \%)}}} \underset{\mathbf{5c}}{\text{Ph–}CH_2CH_2\text{–}CH_2OH} \qquad (10)$$

Selective Conversion of an Alkyl Complex in the Presence of an Acyl Complex. The fact that the dicarbonylalkyl complex **1** was the most reactive of the four types of the organoiron complexes studied (see reaction

---

[11] The reaction of $(\eta^5\text{-}C_5Me_5)Fe(CO)_2$–R was also examined. Thermolysis (90 °C, 6 h) with $HSnMe_3$ gave **5c** (63%), **7** (4%), and **9d** (98%), and photolysis (12 h) with $HSnMe_3$ gave **7** (4%) and **9d** (90%). Thermal reaction with $HSiMe_3$ (100 °C, 3 h) gave R–CH_2SiMe_3 (34%), **5b** (25%), and **7** (22%), and irradiation with $HSiMe_3$ gave **7** (37%) and styrene (50%).

[12] When hydrosilane was used, the silyl group in R–$CH_2OSiR'_3$ was removed by the treatment of the reaction mixture with methanolic KF solution.

[13] **15** does not result from a secondary reaction of **5** with hydrosilane. When the reaction of Fp—CH_2R with H_2SiEt_2 (5 equiv) was carried out in the presence of R—$OSiHEt_2$ (1 equiv), R–H was not formed at all. A plausible mechanism for formation of **15** includes ionization of **25** (Scheme II) by dissociation of ^-OM to give M–Fe^+(H)(=CHR) in which H migration may give M—Fe^+—CH_2R. H transfer from hydrosilane to the cationic alkyl intermediate will form a (hydrido)(alkyl) species like **27**, which reductively eliminates **15**.

[14] Redistribution of H_nSiPh_{4-n} has been frequently observed in transition-metal-catalyzed reactions. See for example; Brown-Wensley, K. A. *Organometallics* **1987**, *6*, 1590.

[15] Fp = $(\eta^5\text{-}C_5H_5)Fe(CO)_2$.

[16] **13** has been found to be active for hydroformylation. Chang, B.; Coil, P. C.; Brown, M. J.; Barnett, K. W. *J. Organomet. Chem.* **1984**, *270*, C23.

Scheme I

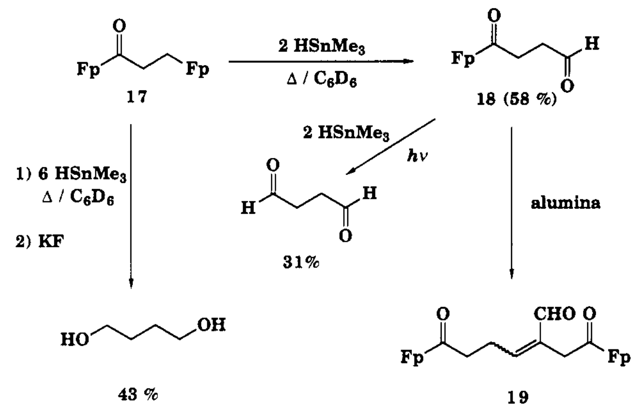

conditions in Table I) prompted us to examine selective conversion of an alkyl complex in the presence of an acyl complex.

Treatment of a 1:1 mixture of $\mathrm{Fp{-}CH_2CH_2CH_2Ph}$ (**16**) and $\mathrm{Fp{-}C(O)CH_2CH_2Ph}$ (**3**) with 2 equiv of $\mathrm{HSnMe_3}$ in benzene for 5 h at 80 °C afforded the products derived from the alkyl complex **16** [$\mathrm{PhCH_2CH_2{-}CHO}$ (88%) and $\mathrm{PhCH_2CH_2{-}CH_2OH}$ (7%)] in preference to **5c** and **6** derived from the acyl complex **3** (eq 11).

$$\underset{\mathbf{16}}{\mathrm{Fp{-}CH_2R}} + \underset{\mathbf{3}}{\mathrm{Fp{-}C(O)R}} + n\mathrm{HSnMe_3} \xrightarrow{80\ ^\circ\mathrm{C,\ benzene}}$$

$$\begin{array}{lccc}
 & \mathrm{RCH_2{-}CHO} + & \mathrm{RCH_2{-}CH_2OH} + & \\
n = 2\ (5\ \mathrm{h}) & 88\% & 7\% & \\
n = 3\ (20\ \mathrm{h}) & 0\% & 66\% & \\
 & \multicolumn{2}{c}{(\text{based on } \mathbf{16})} & \\
 & \underset{\mathbf{6}}{\mathrm{R{-}CHO}} + & \underset{\mathbf{5c}}{\mathrm{R{-}CH_2OH}} + & \mathbf{9a} \\
 & <1\% & 0\% & 42\% \\
 & 24\% & 0\% & 57\% \\
 & \multicolumn{2}{c}{(\text{based on } \mathbf{3})} & (\text{based on } \mathbf{3} + \mathbf{16})
\end{array} \qquad (11)$$

In addition, when (1-oxopropanediyl)diiron complex **17**[17b,c] containing both alkyl and acyl functional groups in the molecule was treated with 2 equiv of $\mathrm{HSnMe_3}$ in benzene for 2 h at 80 °C, the alkyl part selectively reacted to give 1,4-dioxobutyl complex **18** in 58% yield (NMR) accompanied by the formation of **9a** (84%) (Scheme I). Although **18** could be characterized by spectroscopic analyses (see Experimental Section), attempted isolation by column chromatography (alumina) resulted in aldol condensation to give the dinuclear complex **19** (a single isomer). Successive treatment of the reaction mixture containing **18** with an additional 2 equiv of $\mathrm{HSnMe_3}$ under photochemical reaction conditions afforded butanedial in 31% yield based on **17**. On the other hand, the reaction of **17** with 6 equiv of $\mathrm{HSnMe_3}$ for 5 h at 120 °C gave butanediol in 43% yield after treatment with a methanolic KF solution.

However, similar treatment of a μ-ketene diiron complex $\mathrm{Fp{-}CH_2CO{-}Fp}$[17] with $\mathrm{HSnMe_3}$ did not afford **9a** but $\mathrm{Fp{-}SnMe_3}$ (**12a**), and no organic product arising from the ketene part was detected by GLC and NMR analyses. The different behavior should result from the peculiar electronic structure of the μ-ketene complex.[17b,c]

Reaction Mechanism. The formation of the organic products **5**–**8** and organometallic products **9**–**12** by the

Scheme II

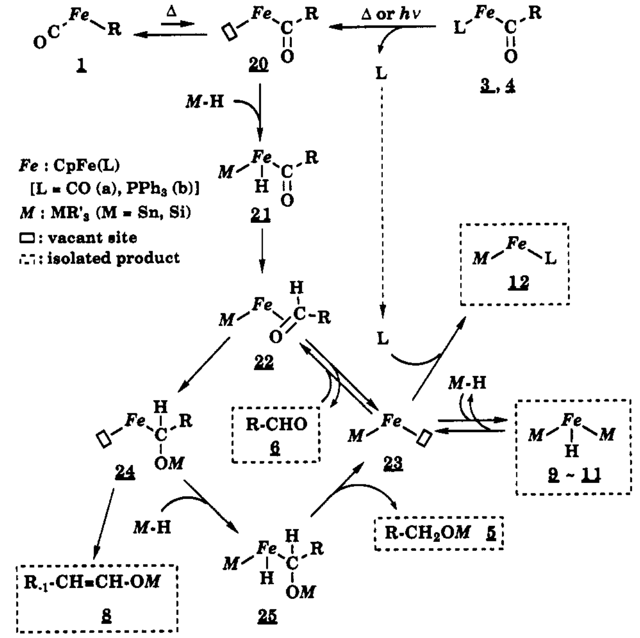

thermal and photochemical reaction of the organoiron complexes **1**–**4** with $\mathrm{HMR'_3}$ may be consistently interpreted by Schemes II, IV, and V.

As shown above the oxymethylation (eq 7) consists of the two consecutive reactions (eqs 5 and 6 and Scheme II). The fact that the alkyl and acyl complexes afford the common product indicates that this reaction is assumed to be initiated by the generation of the coordinatively unsaturated acyl species **20** by either migratory CO insertion of the alkyl complex (**1**) or ligand dissociation from the acyl complexes (**3** and **4**).[18] Judging from the reaction conditions (see Table I, eqs 8 and 9, and Scheme I), this step may be the rate-determining step of the oxymethylation, and the CO insertion appears to be more facile than the ligand dissociation. Oxidative addition of $\mathrm{HMR'_3}$ to **20** gives the (hydrido)(acyl)iron species **21**,[19] from which the aldehyde complex **22** may be formed via reductive elimination. Dissociation of R–CHO (**6**) and oxidative addition of $\mathrm{HMR'_3}$ to the coordinatively unsaturated residue **23** terminates the first step, and the stoichiometry shown in eq 5 is established for the reaction of **1**. The second step is initiated by regeneration of **23** by reductive elimination from **9**–**11**. Coordination of R–CHO (**6**) to give **22** and insertion of **6** into the Fe–M bond in **22** lead to the formation of the coordinatively unsaturated α-(metallooxy)alkyl species **24**. Successive addition of $\mathrm{HMR'_3}$ followed by reductive elimination from the resulting **25**[19] releases the oxymethylated product **5** and **23**, which is finally converted to **9**–**12**. β-Elimination from **24** gives the silyl enol ether **8**. Thus, the second step turns out to be a catalytic reaction with respect to the iron

---

[17] (a) Akita, M.; Kondoh, A.; Moro-oka, Y. *J. Chem. Soc., Chem. Commun.* **1986**, 1296. (b) Akita, M.; Kondoh, A.; Kawahara, T.; Takagi, T.; Moro-oka, Y. *Organometallics* **1988**, *7*, 366. (c) Akita, M.; Kondoh, A.; Moro-oka, Y. *J. Chem. Soc., Dalton Trans.* **1989**, 1083.

[18] See for example: (a) Bibler, J. P.; Wojcicki, A. *Inorg. Chem.* **1966**, *5*, 889. (b) Treichel, P. M.; Subkin, R. L.; Barnett, K. W.; Richard, D. *Inorg. Chem.* **1966**, *5*, 1177. (c) Butler, I. S.; Basolo, F.; Pearson, R. G. *Inorg. Chem.* **1967**, *6*, 2074. (d) Reger, D. L.; Culbertson, E. C. *J. Am. Chem. Soc.* **1976**, *98*, 2789. (e) Kuhlman, E. J.; Alexander, J. J. *Coord. Chem. Rev.* **1980**, *33*, 195. (f) Forschner, T. C.; Cutler, A. R. *Organometallics* **1985**, *4*, 1247. (g) Levitre, S. A.; Tso, C. T.; Cutler, A. R. *J. Organomet. Chem.* **1986**, *308*, 253. (h) Randolph, C. L.; Wrighton, M. S. *J. Am. Chem. Soc.* **1986**, *108*, 3366. (i) Therien, M. J.; Trogler, M. J. *J. Am. Chem. Soc.* **1987**, *109*, 5127. (j) Brunner, H.; Fisch, K. *Angew. Chem., Int. Ed. Engl.* **1990**, *29*, 1131.

[19] Interestingly, the (silyl or stannyl)(hydrido)(organyl)iron(IV) species [**21**, **25** (Scheme II) and **27** (Scheme IV)] reductively eliminate organyl-H rather than $\mathrm{H{-}MR'_3}$.

Scheme III

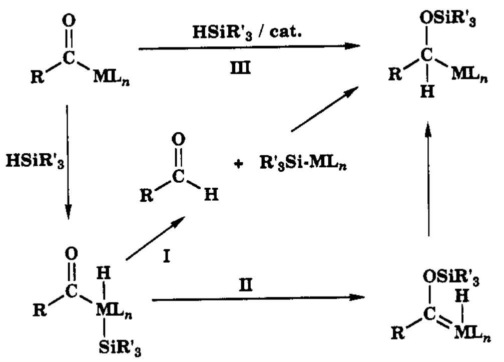

species. Therefore, when a catalytic amount of a coordinatively unsaturated species like **23** is generated in the presence of R–CHO and HMR′$_3$, R–CH$_2$OMR′$_3$ is formed in good yield, as described above.[20]

Recently, Brunner et al.[18j] have reported that the alkyl- and acyliron complexes catalyze hydrosilylation of acetophenone with diphenylsilane. They have also mentioned the following observations: (i) The catalytic activity of the iron complexes correlates with the temperature necessary for epimerization of the starting chiral iron complexes. (ii) When the chiral iron complexes are used as the catalyst, no optical induction is observed. (iii) While Fp–Me is consumed during the catalysis, CpFe(CO)(L)–COCH$_3$ and IndFe(CO)(L)–COCH$_3$ (Ind = η^5-indenyl; L = (*S*)-(+)-Ph$_2$P–N(Me)–CH(Me)Ph) are recovered. (iv) The H–Si bond in diphenylsilane does not oxidatively add to the iron center but interacts with it in the η^2-mode. (v) Therefore, acetophenone does not insert into the Fe–Si bond as usually assumed in the transition-metal-catalyzed hydrosilylation of organic carbonyl compounds but approaches the Si center from the side opposite to the Fe atom. Observations i–iii are in accord with the results of our present study that the formation of the coordinatively unsaturated species is the rate-determining step. The other observations, iii–v, apparently incompatible with our results should come from the dissimilar reaction temperatures. Since we have carried out the reactions at higher temperatures, the Si–H and Sn–H bond should oxidatively add to the iron center.

The mechanism shown in Scheme II resembles a part of the mechanism of the Co$_2$(CO)$_8$-catalyzed oxymethylation studied by Murai et al.[4,21] As a typical example, the oxymethylative opening of oxiranes is shown in eq 12. The ring-opening insertion of the oxirane into

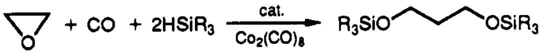

(12)

the highly polarized Si$^{\delta+}$–$^{\delta-}$Co bond in the active species R$_3$SiCo(CO)$_3$ may give the alkyl species R$_3$Si—O(CH$_2$)$_3$—Co(CO)$_4$. Subsequent CO insertion to produce R$_3$Si—O(CH$_2$)$_3$—C(=O)—Co(CO)$_3$ and reduction lead to the formation of the α-siloxyalkyl species R$_3$Si—O(CH$_2$)$_3$—CH(OSiR$_3$)—Co(CO)$_n$ (corresponding to **24**), which releases the diol disilyl ether and R$_3$SiCo(CO)$_4$ by the reaction with HSiR$_3$ and CO. Furthermore, the authors have proposed three possible pathways for conversion of an acylmetal species to an (α-siloxyalkyl)metal species like **24**[4c] (Scheme III: pathway I is similar to Scheme II; pathway II is a 1,3-Si migration to give an α-siloxyalkylidene species followed by H migration;[22] pathway III is a catalytic hydrosilation[5,6]). However, in the present oxymethylation, R–CHO is actually formed in good yield and, therefore, the reaction pathways II and III should be excluded.

Scheme IV

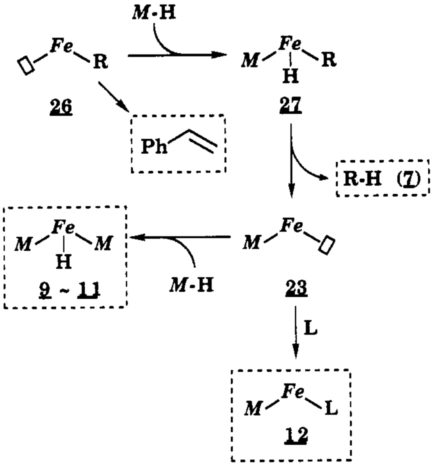

Scheme V

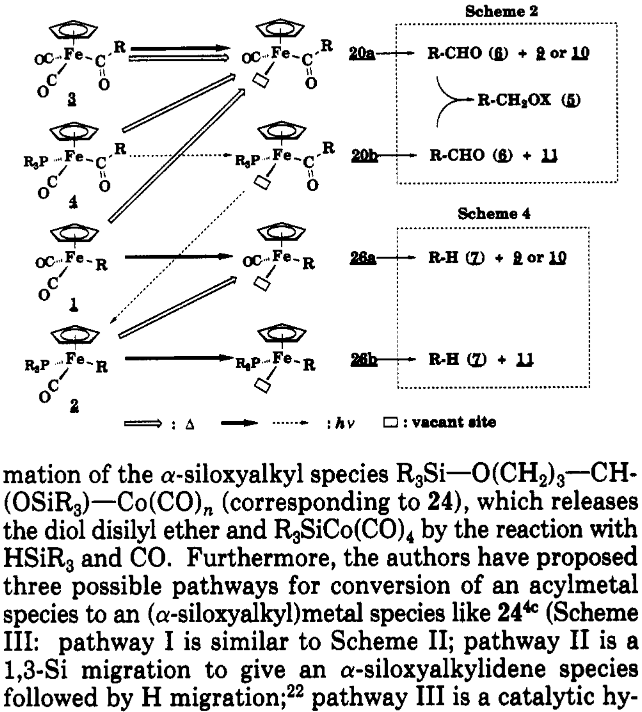

The product distributions observed for the photochemical reactions may be interpreted as follows (Scheme II). Irradiation of **3** may also generate **20**, which is effectively captured by HSnMe$_3$ to give **6** in 79% yield (entry 13 in Table I). Under the photochemical reaction conditions the hydrostannylation of the resulting **6** (eq 6) does not take place because of the lower reaction temperature and, therefore, **5** may not be obtained. On the other hand, the reaction with HSiMe$_3$ affords a mixture of the products (entry 14 in Table I). Two of them (**5** and **8**) derive from **20**, and **7** may be formed via double decarbonylation (**3** → **20** → **1** → **26** → **7**; vide infra).[23] To be noted is that **6** is not detected at all, probably because the insertion of RCHO into the Fe–Si bond may be more facile than that into the Fe–Sn bond due to higher oxygenophilicity of Si,

---

[20] The order of the rate of the catalytic reaction [**9a** > Fp–Me > Fp–C(O)Me ≫ **12a**] may be readily interpreted in terms of the ease of formation of **20**. Surprisingly, Fp$_2$ (**13**), which is finally converted to **12a**, shows a high catalytic activity comparable to **9a**, and no intermediate can be observed by a stoichiometric reaction between **13** and HSnMe$_3$. The active species generated from **13** is not clear until now.

$$\underset{\text{active}}{\mathbf{13}} \xrightarrow{\text{HSnMe}_3} \underset{\text{inactive}}{\mathbf{12a}} \xrightarrow[\#]{\text{HSnMe}_3} \underset{\text{active}}{\mathbf{9a}}$$

[21] (a) Wegman, R. W. *Organometallics* **1986**, *5*, 507. (b) Sisak, A.; Ungvary, F.; Marko, L. *Organometallics* **1986**, *5*, 1019. (b) Kovacs, I.; Sisak, A.; Ungvary, F.; Marko, L. *Organometallics* **1988**, *7*, 1025.

[22] Brinkman, K. C.; Blakeney, A. J.; Krone-Schmidt, W.; Gladysz, J. A. *Organometallics* **1984**, *3*, 1325.

[23] The formation of **7** from **3** and **4** (entries 14 16, Table I) may result from double decarbonylation (**3** → **20a** → **26a**; **4** → **20b** → **2** → **26b**).

Table III. Spectroscopic Data for $CpFe(H)(L)(MR'_3)_2$ (9–11)[a]

		^1H NMR/ppm			^{13}C NMR/ppm			IR/cm^{-1}
complex	MR'_3	H	Cp	R'_3	Cp	CO	R'_3	ν(C≡O)
9a	$SnMe_3$	-13.36 (8.4)[b]	4.07	0.47 (47.7)[b]	79.4 (178.5)[c]	213.1	-3.3 (128.2)[c]	1914
9b	$SnBu_3$	-13.16 *d*	4.25	*e*	78.8 (178.4)[c]	213.5	*e*	1909
9c	$SnPh_3$	-11.29 (15.8)[b]	4.22	7.0–7.8	81.6	212.9	*f*	1935
9d[g]	$SnMe_3$	-12.35 (5.3)[b]	1.56	0.46 (44.9)[b]	10.6, 91.8 (127.2)[c]	215.2	-2.8 (127.2)[c]	1901
10	$SiMe_3$	-13.97	4.04	0.48	83.5 (178.2)[c]	213.9	9.5 (118.8)[c]	1928
10b	$SiEt_3$	-14.05	4.15	0.85–1.16	83.2 (178.3)[c]	214.4	9.6, 13.5 (124.0)[c] (119.2)[c]	1931
10c	$SiHPh_2$	-12.40	4.09		*h*	*h*	*h*	1946
11[i]	$SnMe_3$	-13.28 (36.6)[j] (37.2)[b]	4.05	0.37 (39.7)[b]	77.7 (176.5)[c]		1.27 (126.8)[c]	

[a] Recorded in C_6D_6 at 27 °C. [b] J(H–Sn). [c] J(C–H). [d] Not observed. [e] Bu: 1.02 (CH_3, t, J = 7.3 Hz), 1.21 (CH_2–Sn, t, J = 8.5 Hz), 1.49 (CH_2CH_3, tq, J = 7.3 Hz), 1.65–1.77 ($SnCH_2CH_2$, m), 14.0 (CH_3, q, J = 124.1 Hz), 15.2 (CH_2, t, J = 126.0 Hz), 28.0 (CH_2, t, J = 120.4 Hz), 30.6 (CH_2, t, J = 119.5 Hz). [f] Ph: 128.7, 137.0, 144.0. [g] **9d**: $(\eta^5\text{-}C_5Me_5)Fe(H)(CO)(SnMe_3)_2$. [h] Not recorded. [i] PPh_3: 6.97–7.34. 128.2 (meta or para Ph, d, J(C–H) = 156.3 Hz), 129.5 (meta or para Ph, d, J(C–H) = 158.2 Hz), 133.3 (ortho Ph, dd, J(C–P) = 11.0 Hz, J(C–H) = 158.2 Hz), 139.5 (ipso Ph, d, J(C–P) = 40.4 Hz). [j] J(P–H).

in other words, the reaction path **22** → **23** may be negligible in the case of the reaction with $HSiMe_3$.

Alkane formation may be explained by Scheme IV similar to the mechanism proposed for the photochemical reaction of $(\eta^5\text{-}C_5Me_5)Fe(CO)_2\text{–}Me$ with $HSiMe_3$ by Wrighton et al.[18h] The reaction is initiated by the generation of a coordinatively unsaturated alkyl species **26** by dissociation of a ligand from the alkyl complex **1** and **2**. Sequential addition of HMR'_3, reductive elimination of R–H, and addition of HMR'_3 or L give rise to R–H (**7**) and **9–12**. Styrene may be formed by β-elimination from **26**.

We now postulate a relationship among the organoiron complexes **1–4** and the coordinatively unsaturated acyl and alkyl species **20** and **26**,[18] as shown in Scheme V, on the assumption that a once dissociated ligand does not recombine with any iron species leading to $CpFe(H)(L)(MR'_3)_2$ (**9–11**), in other words, L in **9–11** is bonded to the original iron atom throughout the reaction.[24] Irradiation of **1–4** may result in loss of CO (in preference to PPh_3 for **2** and **4**) to give the corresponding unsaturated species. The parallel relationship (**3** → **20a**, **4** → **20b**,[23] **1** → **26a**, **2** → **26b**) can be seen from Scheme V. On the other hand, thermolysis leads to the formation of **20a** (from **1**, **3**, and **4**) and **26a** (from **2**) via migratory insertion of CO (**1**) or ligand dissociation (**2–4**). In contrast to the photolysis, PPh_3 is lost from the phosphine complexes **2** and **4** in preference to CO. (This consideration is in accord with observation ii by Brunner et al. (vide supra) that the optically active iron complexes racemized via dissociation of the phosphine ligand.[18j]) The generated coordinatively unsaturated species **20** and **26** are readily trapped by HMR'_3 even at room temperature to give the adducts **21** and **27**, respectively, and the final products may be formed according to Schemes II and IV. **20** appears to be formed more readily from the alkyl complex (via migratory CO insertion) than from the acyl complexes (via ligand dissociation). (See eqs 8 and 9 and Scheme I.)

In addition, on the basis of the distribution of the organometallic products **9–12** of the thermal reactions, an order of the apparent reactivity of the 16-electron species $CpFe(CO)(MMe_3)$ (**23**) toward the ligands and HMR'_3 can be estimated as follows: CO > $HSnR'_3$ > PPh_3 > $HSiR'_3$.[25]

Chart I

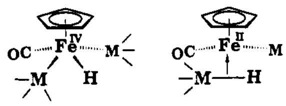

Spectroscopic Characterization of *trans*-$Cp(H)(L)(MR'_3)_2$ (9–11).[26]

The structure of **9** and **10** were readily formulated as $CpFe(H)(CO)(MR'_3)_2$ on the basis of a hydride absorption observed in the range δ -11 to -14, a single CO stretching vibration, and the intensity ratio of the hydride, Cp, and MR'_3 signals (Table III). Analogous complexes, *trans*-$CpFe(H)(CO)(SiX_3)_2$ (X_3 = Cl_3,[27] F_2Me,[28] Me_2Ph[28]), have been already structurally characterized as four-legged piano stool structures with the two SiX_3 groups in the mutually trans two basal positions. The equivalently observed MR'_3 groups in **9** and **10** lead to the conclusion that they also adopt the four-legged piano stool structure with a trans configuration. This conclusion is supported by the structure determination of the $SnPh_3$ derivative (**9c**) by X-ray crystallography (vide infra).

Although Fe(IV) organometallic complexes are very rare,[29] several examples of $(\eta^5\text{-}C_5R_5)Fe(H)(CO)(MR_3)_2$-type compounds, $CpFe(H)(CO)(SiX_3)_2$ (X_3 = Cl_3,[27] F_2Me,[28] Me_2Ph,[28] Et_3[30]) and $(\eta^5\text{-}C_5Me_5)Fe(H)(CO)(SiMe_3)_2$,[18h] have been hitherto reported. They have been prepared by photolysis of Fp_2 or $(\eta^5\text{-}C_5Me_5)Fe(CO)_2\text{–}R$ in the presence

---

[24] This assumption may be supported by the result that **9** (or **10**) and **11** were not formed at the same time under the reaction conditions. (See Table I.)

[25] For example, for entry 5 (Table I), where CO is lost at the initial stage of the reaction, the CO adduct of **23** (**12**) is formed rather than the $HSnMe_3$ adduct **9**. For entries 3 and 7, where PPh_3 is lost, the $HSnMe_3$ adduct **9** is formed rather than the PPh_3 adduct **13**. For entries 2 and 8, where PPh_3 is lost, the PPh_3 adduct **13** is formed in preference to the $HSiMe_3$ adduct **10**. Although we must take into account the fact that some of the organometallic products (e.g. **13a**) do not lose a ligand but some other products (e.g. **9**) reversibly dissociate a ligand under the reaction conditions, the distribution is consistently explained by this order. For a series of the photochemical reactions a different tendency ($HSnMe_3$ > CO > $HSiMe_3$: PPh_3 is not lost under irradiation) has been observed. This may be due to different reaction temperatures and/or secondary reactions.

[26] Preliminary experiments on attempted functionalization of the H–Fe part in **9** were unsuccessful. For example, the reaction with halogen and haloalkanes quantitatively gave Fp–X.

[27] (a) Jetz, W.; Graham, W. A. G. *J. Am. Chem. Soc.* **1969**, *91*, 3375. (b) Jetz, W.; Graham, W. A. G. *Inorg. Chem.* 1971, *10*, 4. (c) Jetz, W.; Graham, W. A. G. *Inorg. Chem.* 1971, *10*, 1159. (d) Manojlovic-Muir, L.; Muir, K. W.; Ibers, J. A. *Inorg. Chem.* **1970**, *9*, 447.

[28] Smith, R. A.; Bennet, M. J. *Acta Crystallogr.* **1977**, *B33*, 1118.

[29] Paciello, R. A.; Manriquez, J. M.; Bercaw, J. E. *Organometallics* **1990**, *9*, 260.

[30] Marinetti-Mignani, A.; West, R. *Organometallics* **1987**, *6*, 141.

Table IV. Crystallographic Data for 9c

formula	$C_{42}H_{36}FeSn_2O$	crys size	0.3 × 0.07 × 0.4
fw	849.97	temp/°C	24
space group	$P\bar{1}$	μ/cm^{-1}	18.05
a/Å	16.248 (7)	transm factor	0.53–1.00
b/Å	19.646 (6)	abs corr	empirical
c/Å	11.443 (5)	2θ/deg	5–54
α/deg	93.32 (3)	no. of reflns collcd	15 659
β/deg	93.67 (4)		
γ/deg	97.09 (3)	no. of unique data with $F > 3\sigma$	8681 (R_{int} = 0.0136)
V/Å^3	3609 (3)		
Z	4		
d_{calc}/g cm^{-3}	1.56	no. of variables	930
F(000)	1688		
		R	0.0312
		R_w	0.0379

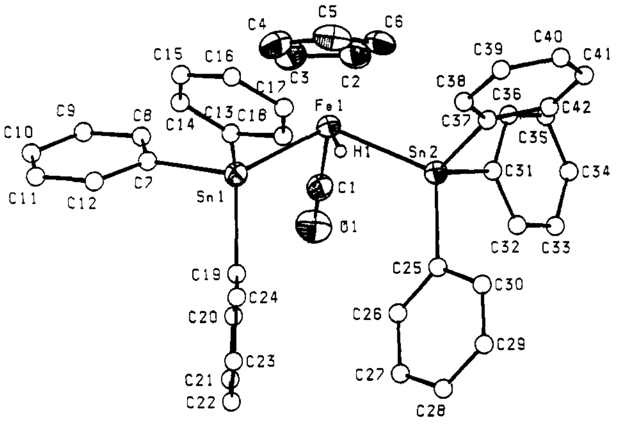

Figure 2. ORTEP drawing of one of the two independentent molecules of 9c.

of the corresponding hydrosilane, and the present thermal and photochemical reaction of the organoiron complexes serves as a complementary preparative method. Wrighton et al. reported that (η^5-C_5Me_5)Fe(H)(CO)($SiMe_3$)$_2$ was unstable due to lability with respect to loss of hydrosilane,[18h] and the silyl complexes (10) obtained by us are also less stable than the stannyl complexes (9).

The interaction between the H and Si atoms in the 10-type complex is still controversial.[31] The structures of 9 and 10 may be described as hybrids of the two extremes, one of which contains a three-center two-electron bond (Chart I). For the silyl complexes, the rather large ^2J(H–Fe–Si) value (20 Hz for the $SiCl_3$ derivative;[23] cf. ^1J(H–Si) ~ 200 Hz for organohydrosilanes) cannot completely exclude the possibility of the η^2-coordination of the H–Si bond. However, such contribution is negligible for the stannyl complexes on the basis of the magnitude of the ^2J(H–Fe–Sn) values of the stannyl complexes (**9a**, 8.4 Hz; **9c**, 15.8 Hz; **9d**, 5.3 Hz)[32] compared to the ^1J(H–Sn) values of organohydrostannanes (1500–1975 Hz).[33]

The structure of the phosphine-substituted analogue (**11**) was also assigned to *trans*-CpFe(H)(PPh_3)($SnMe_3$)$_2$ on the basis of its ^{1}H NMR data. Although its ^2J(H–Fe–Sn) value (37 Hz) is the largest of the 9-type complexes obtained, the magnitude is still not enough to demonstrate the η^2-coordination mode.

Molecular Structure of CpFe(H)(CO)(SnPH$_3$)$_2$ (9c). The asymmetric unit contains two crystallographically independent molecules of the essentially same geometry. The crystal data, positional parameters, and selected bond lengths and angles are listed in Tables IV–VI. An ORTEP drawing of one of the two molecules is reproduced in Figure 2, and bottom view of the core part of the two molecules are shown in Figure 3.

Scheme VI

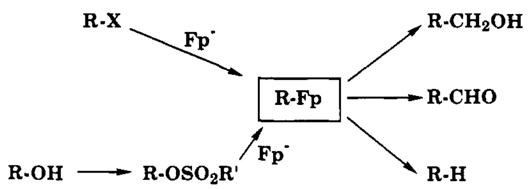

Scheme VII

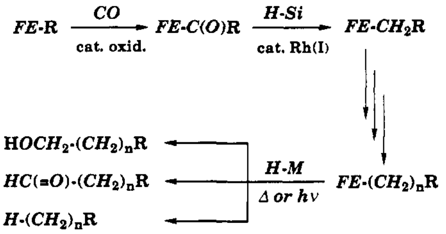

The overall geometry of **9c**, which is consistent with the spectroscopic analyses, can be described as the four-legged piano stool structure with the trans configuration with respect to the two $SnPh_3$ groups. The structural parameters of **9c** are compared with related compounds, i.e., the silyl analogues CpFe(H)(CO)(SiX_3)$_2$ (X_3 = Cl_3,[27] F_2Me,[28] Me_2Ph[28]), a stannyliron(II) complex Fp–$SnPh_3$,[34] and a typical organoiron complex Fp–$CH_2CH_2C(O)$–Fp (**17**)[17c] (Table VII). The parameters for the CpFe(CO)$_n$ part and the interligand angles are essentially the same irrespective of M and R. The Fe–Sn distances fall in the range of those of previously reported complexes (Fe–Sn = 2.47–2.67 Å).[33] The dihedral angle between the two Cp–Fe–Sn planes is 144.3°, which results from minimization of the steric repulsion due to the bulky $SnPh_3$ groups. The hydride ligand can be located in a basal position trans to CO and is about equidistant from the two Sn atoms (H(1)–Sn(1) = 2.31 (4) Å, H(1)–Sn(2) = 2.22 (4) Å, H(2)–Sn(3) = 2.21 (4) Å, H(2)–Sn(4) = 2.28 Å). These structural features also lead to the conclusion that, at least for **9c**, the η^2-coordination mode of the H–Sn bond is negligible.

Conclusion

Extensive studies on the chemistry of the half-sandwich organoiron complexes, CpFe(CO)(L)–alkyl and –acyl, have revealed that their accessibility as well as thermal stability merit their utilization as a versatile stoichiometric reagent for various transformations of the organic ligand.[35] However, little attention has been paid to reductive cleavage of such compounds.[36] Herein we have described transformation of the organoiron complexes 1–4 into R–CH_2OH, R–CHO, and R–H under thermal and photochemical reaction conditions. Since 1 is readily prepared by the reaction of R–X with Fp^-, the Fp^- reagent turns out to serve as an equivalent to $^-CH_2OH$, ^-CHO, and H^- with nucleophilic character, as shown in Scheme VI. In addition, alcohol (R–OH) may be converted to R–Fp by way of a sulfonic acid ester (R–OSO_2R') and, therefore, Fp^- may also serve as an alcohol-homologating reagent.

In principle, combination of the present reaction and the previously reported Rh(I)-catalyzed hydrosilylation[5] will provide a model system for surface-catalyzed hydro-

---

(31) Schubert, U. *Adv. Organomet. Chem.* **1990**, *30*, 151.

(32) The satellite peaks due to ^2J(H–Fe–Sn) were not observed for **9b**.

(33) Davies, A. G.; Smith, P. J. In *Comprehensive Organometallic Chemistry*; Wilkinson, G., Stone, F. G. A., Eds.; Pergamon Press: Oxford, U.K. 1982; Vol. 2, Chapter 11, p 586.

(34) Bryan, R. F. *J. Chem. Soc. A* **1967**, 192.

(35) See for example: Rosenblum, M. *J. Organomet. Chem.* **1986**, *300*, 191.

(36) Wong, A.; Atwood, J. D. *ACS Symp. Ser.* **1981**, *152*, 265.

Table V. Positional Parameters for Non-Hydrogen Atoms of 9c

atom	*x*	*y*	*z*	*B*(eq)/Å^2	atom	*x*	*y*	*z*	*B*(eq)/Å^2
Sn(1)	0.98397 (2)	0.35937 (1)	0.79895 (2)	3.53 (1)	C(40)	0.8175 (4)	0.0913 (3)	1.2399 (5)	7.3 (3)
Sn(2)	1.03061 (2)	0.17457 (1)	0.97481 (2)	3.34 (1)	C(41)	0.8922 (4)	0.0680 (3)	1.2413 (5)	6.6 (3)
Sn(3)	0.48502 (2)	0.36409 (2)	0.29259 (3)	3.98 (1)	C(42)	0.9497 (3)	0.0916 (2)	1.1669 (4)	5.3 (2)
Sn(4)	0.52743 (2)	0.17875 (2)	0.47076 (2)	3.63 (1)	C(43)	0.6303 (3)	0.2902 (2)	0.3561 (4)	4.6 (2)
Fe(1)	1.05836 (4)	0.30582 (3)	0.96766 (5)	3.46 (2)	C(44)	0.5090 (4)	0.3594 (3)	0.5971 (4)	6.2 (3)
Fe(2)	0.56135 (4)	0.30925 (3)	0.45852 (5)	3.85 (3)	C(45)	0.5545 (4)	0.3096 (3)	0.6420 (4)	6.2 (3)
O(1)	1.1834 (2)	0.2816 (2)	0.8063 (3)	6.3 (2)	C(46)	0.6368 (4)	0.3254 (3)	0.6141 (4)	6.3 (3)
O(2)	0.6798 (2)	0.2797 (2)	0.2907 (3)	7.0 (2)	C(47)	0.6431 (4)	0.3858 (3)	0.5530 (5)	6.6 (3)
C(1)	1.1313 (3)	0.2903 (2)	0.8693 (4)	4.3 (2)	C(48)	0.5632 (4)	0.4065 (3)	0.5431 (5)	6.8 (3)
C(2)	1.1343 (3)	0.3288 (3)	1.1210 (4)	5.6 (2)	C(49)	0.5472 (3)	0.4622 (2)	0.2465 (4)	4.5 (2)
C(3)	1.1274 (4)	0.3882 (3)	1.0638 (4)	6.8 (3)	C(50)	0.6254 (3)	0.4896 (3)	0.2935 (5)	6.6 (3)
C(4)	1.0420 (4)	0.3980 (3)	1.0573 (4)	7.5 (3)	C(51)	0.6633 (4)	0.5522 (3)	0.2609 (6)	7.5 (3)
C(5)	0.9989 (4)	0.3433 (3)	1.1103 (4)	7.1 (3)	C(52)	0.6251 (4)	0.5873 (3)	0.1798 (5)	7.0 (3)
C(6)	1.0557 (3)	0.3014 (3)	1.1499 (4)	5.6 (2)	C(53)	0.5467 (4)	0.5620 (3)	0.1353 (5)	7.2 (3)
C(7)	1.0450 (3)	0.4591 (2)	0.7577 (4)	4.3 (2)	C(54)	0.5082 (3)	0.4990 (3)	0.1663 (5)	5.9 (3)
C(8)	1.1217 (3)	0.4870 (3)	0.8052 (5)	6.5 (3)	C(55)	0.3632 (3)	0.3794 (2)	0.3475 (4)	4.3 (2)
C(9)	1.1605 (3)	0.5491 (3)	0.7715 (6)	7.5 (3)	C(56)	0.3277 (3)	0.4383 (2)	0.3330 (4)	4.7 (2)
C(10)	1.1222 (4)	0.5827 (3)	0.6873 (5)	6.5 (3)	C(57)	0.2492 (3)	0.4454 (3)	0.3708 (5)	5.9 (3)
C(11)	1.0458 (4)	0.5570 (3)	0.6401 (5)	6.8 (3)	C(58)	0.2072 (3)	0.3929 (3)	0.4249 (5)	6.7 (3)
C(12)	1.0066 (3)	0.4945 (3)	0.6741 (4)	5.7 (2)	C(59)	0.2406 (3)	0.3343 (3)	0.4401 (5)	6.9 (3)
C(13)	0.8595 (3)	0.3712 (2)	0.8445 (4)	4.0 (2)	C(60)	0.3178 (3)	0.3264 (3)	0.4003 (5)	6.6 (3)
C(14)	0.8281 (3)	0.4332 (2)	0.8486 (4)	5.1 (2)	C(61)	0.4596 (3)	0.3028 (2)	0.1279 (4)	4.2 (2)
C(15)	0.7494 (3)	0.4379 (3)	0.8840 (5)	6.3 (3)	C(62)	0.5232 (3)	0.2889 (3)	0.0590 (4)	5.3 (2)
C(16)	0.7003 (3)	0.3819 (3)	0.9154 (5)	6.6 (3)	C(63)	0.5052 (3)	0.2490 (3)	-0.0456 (4)	6.5 (3)
C(17)	0.7305 (3)	0.3190 (3)	0.9108 (6)	7.4 (3)	C(64)	0.4257 (4)	0.2222 (3)	-0.0793 (4)	6.4 (3)
C(18)	0.8083 (3)	0.3135 (3)	0.8757 (5)	6.0 (3)	C(65)	0.3630 (3)	0.2352 (3)	-0.0120 (5)	6.7 (3)
C(19)	0.9668 (3)	0.3037 (2)	0.6295 (3)	3.8 (2)	C(66)	0.3798 (3)	0.2762 (3)	0.0919 (5)	5.5 (2)
C(20)	1.0347 (3)	0.2922 (3)	0.5659 (4)	5.2 (2)	C(67)	0.5474 (3)	0.1161 (2)	0.3183 (4)	4.0 (2)
C(21)	1.0224 (3)	0.2600 (3)	0.4550 (4)	5.9 (3)	C(68)	0.5226 (3)	0.1316 (3)	0.2063 (4)	5.4 (2)
C(22)	0.9450 (3)	0.2378 (3)	0.4065 (4)	6.0 (2)	C(69)	0.5357 (4)	0.0892 (3)	0.1108 (4)	6.7 (3)
C(23)	0.8783 (3)	0.2488 (3)	0.4667 (4)	6.5 (3)	C(70)	0.5747 (3)	0.0326 (3)	0.1237 (4)	6.1 (3)
C(24)	0.8890 (3)	0.2817 (3)	0.5783 (4)	5.5 (2)	C(71)	0.5992 (3)	0.0162 (3)	0.2338 (5)	5.5 (2)
C(25)	0.9916 (3)	0.1173 (2)	0.8114 (4)	3.6 (2)	C(72)	0.5848 (3)	0.0574 (2)	0.3305 (4)	4.9 (2)
C(26)	1.0216 (3)	0.1348 (2)	0.7051 (4)	4.8 (2)	C(73)	0.4027 (3)	0.1440 (2)	0.5142 (4)	3.9 (2)
C(27)	0.9935 (3)	0.0962 (3)	0.6019 (4)	5.6 (2)	C(74)	0.3637 (3)	0.0796 (2)	0.4721 (4)	4.6 (2)
C(28)	0.9360 (3)	0.0400 (3)	0.6029 (4)	5.2 (2)	C(75)	0.2860 (3)	0.0541 (3)	0.5015 (5)	5.8 (3)
C(29)	0.9055 (3)	0.0214 (2)	0.7074 (4)	5.0 (2)	C(76)	0.2432 (3)	0.0928 (3)	0.5736 (5)	6.6 (3)
C(30)	0.9330 (3)	0.0591 (2)	0.8097 (4)	4.3 (2)	C(77)	0.2787 (3)	0.1573 (3)	0.6154 (5)	6.8 (3)
C(31)	1.1405 (3)	0.1345 (2)	1.0415 (4)	4.1 (2)	C(78)	0.3588 (3)	0.1828 (3)	0.5870 (5)	5.4 (2)
C(32)	1.1742 (3)	0.0854 (3)	0.9753 (5)	5.8 (3)	C(79)	0.6077 (3)	0.1454 (2)	0.6076 (4)	3.8 (2)
C(33)	1.2426 (4)	0.0568 (3)	1.0171 (6)	8.2 (4)	C(80)	0.5765 (3)	0.1158 (3)	0.7028 (4)	5.8 (3)
C(34)	1.2803 (3)	0.0773 (3)	1.1259 (6)	8.0 (3)	C(81)	0.6294 (4)	0.0962 (3)	0.7919 (5)	7.7 (3)
C(35)	1.2481 (3)	0.1258 (3)	1.1948 (5)	6.8 (3)	C(82)	0.7128 (4)	0.1052 (3)	0.7851 (5)	6.9 (3)
C(36)	1.1788 (3)	0.1537 (3)	1.1535 (4)	5.5 (2)	C(83)	0.7458 (3)	0.1334 (3)	0.6891 (5)	6.4 (3)
C(37)	0.9361 (3)	0.1423 (2)	1.0910 (4)	3.9 (2)	C(84)	0.6928 (3)	0.1535 (3)	0.6006 (4)	5.4 (2)
C(38)	0.8598 (3)	0.1656 (3)	1.0901 (4)	5.9 (3)	H(1)	0.981 (2)	0.272 (2)	0.924 (3)	3.6 (8)
C(39)	0.7998 (3)	0.1402 (3)	1.1659 (5)	7.1 (3)	H(2)	0.482 (2)	0.277 (2)	0.407 (3)	4.3 (9)

genation of CO (Scheme VII). As reported earlier, carbonylation of a phosphine-substituted alkyliron complex, $CpFe(CO)(PPh_3)$–R, by the action of a catalytic amount of oxidant gives $CpFe(CO)(PPh_3)$–C(O)R, which can be reduced to the homologated alkyl complex $CpFe(CO)(PPh_3)$–CH_2R by $H_2SiR'_2$ in the presence of a Rh(I) catalyst. Repetition of this cycle will afford $CpFe(CO)(PPh_3)$–$(CH_2)_nR$. Treatment of the resulting complex with HMR'_3 under thermal or photochemical reaction conditions produces $R(CH_2)_nCH_2OH$ or R–CHO or $R(CH_2)_nH$, in which all the carbon atoms and the hydrogen atoms except the OH proton originate from CO and HMR'_3, respectively.

In addition, we have isolated a series of $CpFe(H)(L)(MR'_3)_2$ complexes (L = CO, PPh_3) and determined the molecular structure of **9c**. The spectroscopic as well as structural features indicate that the contribution of the η^2-Sn–H coordination mode is negligible.

Experimental Section

All manipulation was carried out under an argon atmosphere by using standard Schlenk tube technique.

Benzene was dried over Na–K/benzophenone, distilled, and stored under an argon atmosphere. Benzene-d_6 containing 0.5% TMS was dried over molecular sieves and distilled under reduced pressure. Fp–alkyl and –acyl complexes including **1**, **3**, and **16** were prepared by the reaction of NaFp with appropriate alkyl halides and acid chlorides.[37] **4** was prepared by the reaction of **1** with PPh_3 in refluxing acetonitrile.[18a] **2** was prepared by the reaction of $CpFe(CO)(PPh_3)I$ with RLi.[38] The dinuclear complexes, **17** and Fp–$CH_2C(O)$–Fp, were prepared according to our previous report.[17b] Structures of the organometallic products **12a–d**,[39] **13**, and $[CpFe(CO)]_4$,[40] were identified by comparison of the spectral data with those of the authentic samples. Hydrostannanes and -silanes except $HSnBu_3$, $HSnPh_3$, and $HSiPh_3$ (purchased) were prepared by the reaction of appropriate halides with $LiAlH_4$. The authentic samples of **5b**, **8**,[41] butanedial,[42] and $PhCH_2CH_2CH_2CHO$[43] were prepared by the established methods. Other organic reagents were purchased and used as received.

^1H and ^{13}C NMR spectra were recorded on Hitachi R-24B, JEOL EX-90, and JEOL GX-270 spectrometers. IR spectra were obtained on a Hitachi 26-50 spectrometer. The GLC analyses

---

[37] King, R. B. *Organometallic Synthesis*; Academic Press: New York, 1965; Vol. 1.

[38] Reger, D. L.; Culbertson, E. C. *Synth. React. Inorg. Met-Org. Chem.* **1976**, *6*, 1.

[39] King, R. B.; Pannell, K. H. *Inorg. Chem.* **1968**, *7*, 1510.

[40] King, R. B. *Inorg. Chem.* **1966**, *5*, 2227.

[41] Suzuki, H.; Koyama, Y.; Moro-oka, Y.; Ikawa, T. *Tetrahedron Lett.* **1979**, 1415.

[42] Fakstord, J.; Raleigh, D.; Schniepp, L. E. *J. Am. Chem. Soc.* **1950**, *72*, 869.

[43] The aldehyde was prepared by oxidation of $Ph(CH_2)_4OH$ by PCC. D'auria, M. *Synthesis* **1982**, 245.

Table VI. Selected Bond Lengths (Å) and Angles (deg) for 9c[a]

molecule 1		molecule 2	
	Bond Lengths		
C–C(Cp)	1.383 (9)–1.423 (9)	C–C(Cp)	1.396 (8)–1.407 (9)
Fe1–C(Cp)	2.068 (5)–2.095 (5)	Fe2–C(Cp)	2.081 (5)–2.109 (5)
Fe1–CP1	1.701	Fe2–CP2	1.671
Fe1–H1	1.40 (3)	Fe2–H2	1.43 (3)
Fe1–Sn1	2.558 (1)	Fe2–Sn3	2.563 (1)
Fe1–Sn2	2.569 (1)	Fe2–Sn4	2.569 (1)
Fe1–C1	1.728 (5)	Fe2–C43	1.729 (5)
C1–O1	1.168 (6)	C43–O2	1.161 (6)
Sn1–C7	2.176 (4)	Sn3–C49	2.173 (5)
Sn1–C13	2.157 (5)	Sn3–C55	2.165 (5)
Sn1–C19	2.155 (4)	Sn3–C61	2.164 (4)
Sn2–C25	2.143 (4)	Sn4–C67	2.141 (4)
Sn2–C31	2.152 (5)	Sn4–C73	2.155 (4)
Sn2–C37	2.155 (4)	Sn4–C79	2.156 (4)
C–C(Ph)	1.347 (8)–1.401 (8)	C–C(Ph)	1.346 (9)–1.400 (8)
	Bond Angles		
C–C–(Cp)	107.3 (5)–108.7 (5)	C–C–C(Cp)	107.0 (5)–108.4 (5)
Cp1–Fe1–H1	119.7	CP2–Fe2–H2	125.3
CP1–Fe1–Sn1	115.9	CP2–Fe2–Sn3	117.4
CP1–Fe1–Sn2	115.6	CP2–Fe2–Sn4	113.9
CP1–Fe1–C1	109.8	CP2–Fe2–C43	104.9
H1–Fe1–Sn1	63 (2)	H2–Fe2–Sn3	59 (2)
H1–Fe1–Sn2	61 (2)	H2–Fe2–Sn4	63 (2)
H1–Fe1–C1	109 (2)	H2–Fe2–C43	104 (2)
Sn1–Fe1–Sn2	117.10 (4)	Sn3–Fe2–Sn4	117.21 (4)
Sn1–Fe1–C1	85.9 (2)	Sn3–Fe2–C43	86.1 (2)
Sn2–Fe1–C1	85.9 (2)	Sn4–Fe2–C43	86.3 (2)
Fe1–C1–O1	176.9 (4)	Fe2–C43–O2	176.4 (4)
Fe1–Sn1–C7	114.1 (1)	Fe2–Sn3–C49	114.5 (1)
Fe1–Sn1–C13	108.6 (1)	Fe2–Sn3–C55	107.8 (1)
Fe1–Sn1–C19	118.3 (1)	Fe2–Sn3–C61	116.2 (1)
C7–Sn1–C13	108.4 (2)	C49–Sn3–C55	108.4 (2)
C7–Sn1–C19	102.3 (2)	C49–Sn3–C61	105.0 (2)
C13–Sn1–C19	104.3 (2)	C55–Sn4–C61	104.2 (2)
Fe1–Sn2–C25	116.4 (1)	Fe2–Sn4–C67	116.3 (1)
Fe1–Sn2–C31	110.6 (1)	Fe2–Sn4–C73	115.3 (1)
Fe1–Sn2–C37	113.0 (1)	Fe2–Sn4–C79	109.3 (1)
C25–Sn2–C31	106.1 (2)	C67–Sn4–C73	105.5 (2)
C25–Sn2–C37	104.7 (2)	C67–Sn4–C79	104.0 (2)
C31–Sn1–C37	105.3 (2)	C73–Sn4–C79	105.3 (2)
C–C–C(Ph)	117.1 (4)–121.7 (5)	C–C–C(Ph)	116.9 (4)–122.4 (5)

[a] CP1 and CP2 are the centroid of C2–C6 and C44–C48, respectively.

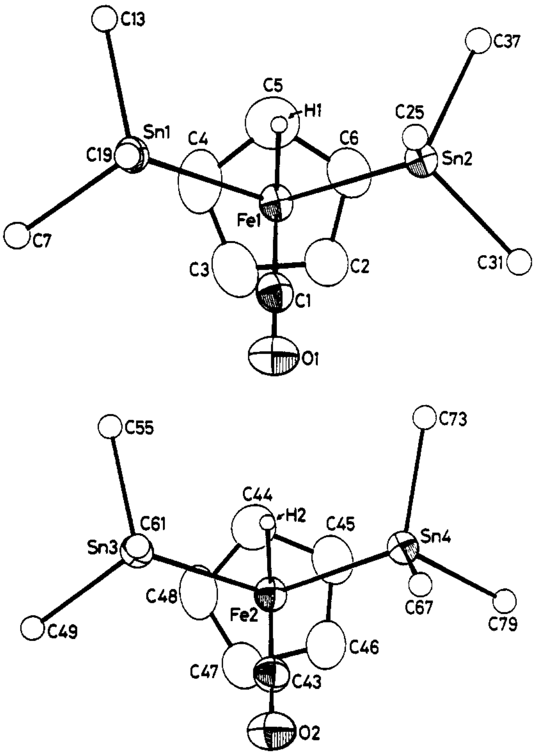

Figure 3. Core structures of **9c**: (top) molecule 1; (bottom) molecule 2.

of the reaction products were made on a Hitachi 163 gas chromatograph using a column packed with PEG 20M (the experiments for Table II) and silicon SE-30 (others). MS spectra were obtained on a Hitachi M-80 mass spectrometer using a GLC column packed with silicon SE-30. All the organic products were identified by GCMS analyses as well as comparison of the GLC retention time with those of authentic samples. Column chromatography was performed on alumina (activity II–IV, Merck Art. 1097).

Thermal Reaction of Organoiron Complexes 1–4. (a) NMR Experiments. An iron complex (0.10 mmol) was weighed in an

Table VII. Structural Parameters for Fe–M Complexes

complex	Fe–CP[a]	Fe–CO	C–O	Fe–M(R)	Fe–H	⟨CP–Fe–CO	⟨CP–Fe–M(R)	⟨M–Fe–CO
9c	1.701[b]	1.728 (5)	1.168 (6)	2.558 (1)	1.40 (3)	130.4	115.6	85.9 (2)
				2.569 (1)			115.9	85.9 (2)
	1.671[c]	1.729 (5)	1.161 (6)	2.563 (1)	1.43 (3)	129.8	113.9	86.1 (2)
				2.569 (1)			117.4	86.3 (2)
$SiCl_3$[d]	1.718	1.758 (9)	1.132 (10)	2.252 (3)	*e*	125.8	118.1	84.4 (3)
				2.252 (3)			119.4	85.1 (3)
SiF_2Me[f,g]	1.72	1.73 (1)	1.156 (4)	2.249 (1)	1.49 (6)	129.5	119.4	82.6
$SiMe_2Ph$[h]	1.72	1.71 (1)	*e*	2.336	*e*	*e*	*e*	*e*
Fp–Sn[i]	1.73[b]	1.70	1.19	2.533		126	124	84
		1.74	1.16			128		89
	1.72[c]	1.71	1.17	2.540		126	120	85
		1.73	1.15			127		88
17	1.732[j]	1.739 (6)	1.152 (8)	2.071 (5)		128.2	121.3	88.3 (3)
		1.750 (7)	1.140 (9)			125.2		88.7 (3)
	1.738[k]	1.744 (8)	1.150 (10)	1.992 (5)		121.3	117.9	88.7 (2)
		1.753 (6)	1.152 (7)			127.4		94.3 (3)

complex	⟨M–Fe–M	⟨H–Fe–CO	CP–Fe–M[l] CP–Fe–M′	CP–Fe–M[l] CP–Fe–CO	CP–Fe–M[l] CP–Fe–H	CP–Fe–H[l] CP–Fe–CO
9c	117.10 (4)	108.6	144.3	107.1	71.6	178.1
			108.5	72.7		
	117.21 (4)	104.1	144.3	107.0	69.6	178.6
			108.7	74.7		
$SiCl_3$	115.3	*e*	106.6	*e*	*e*	
			104.4			
SiF_2Ph	113.9 (1)	106.6	148.4	105.8	74.2	180.0

[a] CP is the centroid of the Cp ring. [b] One of the two independent molecules. [c] The other independent molecule. [d] $SiCl_3$: $CpFe(H)(CO)(SiCl_3)_2$. [e] Not available. [f] SiF_2Me: $CpFe(H)(CO)(SiF_3Me)_2$. [g] The molecule has a plane of symmetry. [h] $SiMe_2Ph$: $CpFe(H)(CO)(SiMe_3Ph)_2$. [i] $CpFe(CO)_2–SnPh_3$. [j] The Fp–CH_2 part. [k] The Fp–C(O) part. [l] Dihedral angle.

NMR tube, which was evacuated and refilled with argon. C_6D_6 (0.4 mL) and HMR'_3 (0.30 mmol) were added to the tube by syringes. Then the tube was sealed and heated in a temperature-controlled oil bath or a GLC oven under conditions described in Table I. Yields of the organic products were determined by GLC after addition of appropriate internal standards (acenaphthene for **5b**,**c**, and **8**; *n*-dodecane for **6**; toluene for **7**). Other reactions were carried out similarly. Yields of organometallic products formed by the reaction with $HSnR'_3$ were directly determined by ^1H NMR spectroscopy. However, those formed by the reaction with $HSiR'_3$ were determined after filtration through an alumina plug because of broadening of the spectra.

(b) Isolation of 9 and 10. 9a. To **1** (2.00 g, 7.1 mmol) dissolved in 10 mL of benzene in a glass tube was added $HSnMe_3$ (3.3 mL, 21.3 mmol). After the tube was closed with a screw cap, the tube was placed in an oil bath heated at 90 °C. After 3 h the consumption of **1** was checked by TLC, and then the volatiles were removed under reduced pressure. **9a** was isolated by column chromatography. Elution with hexanes gave a yellow band, from which **9a** (2.98 g, 6.25 mmol, 88%) was isolated as a yellow oil. An analytically pure sample was obtained by distillation under reduced pressure.

9c. 1 (560 mg, 2.00 mmol) and $HSnPh_3$ (2.10 g, 6.00 mmol) were heated in benzene (10 mL) for 2 h at 120 °C as described above. Separation by column chromatography (eluted with hexanes:CH_2Cl_2 = 5:1) followed by twice-repeated recrystallization from hexanes–CH_2Cl_2 gave an analytically pure sample of **9c** (341 mg, 0.40 mmol, 20% yield) as yellow plates.

Other **9** and **10** were prepared in a similar manner. **10a** and **9b**,**d** were purified by distillation and passage through an alumina column, respectively, but pure samples of **10b**,**c** were not obtained. Anal. Calcd for $C_{12}H_{24}FeSn_2O$ (**9a**): C, 30.18; H, 5.07. Found: C, 30.11; H, 5.25. Calcd for $C_{30}H_{60}FeSn_2O$ (**9b**): C, 49.36; H, 8.28. Found: C, 49.07; H, 8.74. Calcd for $C_{42}H_{36}FeSn_2O$ (**9c**): C, 59.35; H, 4.27. Found: C, 59.24; H, 4.11. Calcd for $C_{17}H_{29}FeSn_2O$ (**9d**): C, 37.28; H, 6.24. Found: C, 37.46; H, 6.07. Calcd for $C_{12}H_{24}FeSi_2O$ (**10a**): C, 48.64; H, 8.16. Found: C, 48.54; H, 8.41.

Photochemical Reaction of Organoiron Complexes with $HMMe_3$. An NMR sample was prepared as described for the thermal reaction and irradiated by a high-pressure mercury lamp. The reaction was monitored by ^1H NMR spectroscopy at appropriate intervals.

Preparation of 11 by Photolysis of 4 with $HSnMe_3$. A benzene solution (5.0 mL) of **11** (544.4 mg, 1.00 mmol) and $HSnMe_3$ (0.45 mL, 3.00 mmol) in a quartz reaction tube was photolyzed by a high-pressure mercury lamp for 2 days. After the consumption of **4** was checked by TLC, the volatiles were removed under reduced pressure. Column chromatography eluted with hexanes gave an orange band, from which **11** (306.3 mg, 0.430 mmol, 43% yield) was isolated as brown crystals after recrystallization from CH_2Cl_2–hexanes. Anal. Calcd for $C_{29}H_{39}FeSn_2P$ (**11**): C, 48.93; H, 5.52. Found: C, 49.59; H, 5.55.

Selective Conversion of 16 in the Presence of 3. An NMR tube containing **16** (29.6 mg, 0.10 mmol) and **3** (31.0 mg, 0.10 mmol), $HSnMe_3$ (30 μL, 0.20 mmol or 46 μL, 0.30 mmol), and C_6D_6 (0.4 mL) was prepared as described above and heated at 80 °C.

Reaction of 17. A sealed NMR tube containing **17** (41.0 mg, 0.10 mmol), $HSnMe_3$ (30 μL, 0.20 mmol), and C_6D_6 (0.4 mL) was heated for 2 h at 80 °C. Formation of **18** (58% yield) and **9a** (84%) was confirmed by ^1H NMR spectroscopy. Then the tube was opened, $HSnMe_3$ (30 μL, 0.20 mmol) was added, and the tube was sealed again. After photolysis of the sample for 3 h butanedial (31%) was formed. **18**: ^1H NMR (C_6D_6) δ 2.06 (2 H, t, J = 5.9 Hz, CH_2), 2.85 (2 H, t, J = 5.9 Hz, CH_2), 4.24 (5 H, s, Cp), 9.31 (1 H, s, CHO); IR (CH_2Cl_2) 2014, 1958 ($\nu_{C\equiv O}$), 1722 ($\nu_{CH=O}$), 1639 ($\nu_{Fe-C=O}$).

Attempted isolation of **18** by column chromatography resulted in aldol condensation to give **19**, a pure sample of which was not obtained. **19**: ^1H NMR (C_6D_6) δ 1.97 (2 H, dt, J = 7.8 and 7.1 Hz, $CH_2{=}CH$), 2.58 (2 H, t, J = 7.1 Hz, $C(O){-}CH_2CH_2$), 3.57 (2 H, s, $C(O){-}CH_2$), 3.97 (5 H, s, Cp), 4.05 (5 H, s, Cp), 5.88 (1 H, t, J = 7.8 Hz, $={-}CH$), 8.87 (1 H, s, CHO); ^{13}C NMR (C_6D_6) δ 25.9 ($CH_2{-}CH{=}$), 60.4 ($Fp{-}C(O)CH_2CH_2$), 63.4 ($={-}CCH_2C(O){-}Fp$), 86.2 (Cp), 86.4 (Cp), 139.4 ($CH{=}C<$), 154.4 ($CH{=}C<$), 193.7 (CHO), 214.9 (CO), 215.0 (CO), 248.4 ($Fe{-}C(O)$), 250.5 ($Fe{-}C(O)$); IR (KBr) 2008, 1962, 1939, 1671, 1628 cm^{-1}.

The reaction of **17** (205.0 mg, 0.50 mmol) with $HSnMe_3$ (0.46 mL, 3.0 mmol) for 5 h at 120 °C gave butanediol in 43% yield after addition of a solution of KF (35.0 mg, 0.60 mmol) in MeOH (0.6 mL) and H_2O (2.0 mL).

Hydrostannylation of R–CHO Catalyzed by Iron Complexes. To a glass tube that was flashed with argon were added $PhCH_2CH_2CHO$ (132 μL, 1.00 mmol), $HSnMe_3$ (153 μL, 1.00 mmol), an iron complex (0.1 mmol; Fp_2 0.05 mmol), benzene (1.0 mL), and *n*-dodecane (91 μL, 0.40 mmol) (internal standard). Then the tube was closed with a screw cap and heated at 120 °C. The reaction was monitored by GLC at appropriate intervals.

Crystallographic Analysis. A yellow plate of **9c** obtained by recrystallization from CH_2Cl_2–hexanes was mounted on a glass fiber. Diffraction measurement was made on a Rigaku AFC-5R automated four-circle diffractometer by using graphite-monochromated Mo Kα radiation (λ = 0.710690 Å). The unit cell was determined by a least-squares method by using 24 selected reflections. Crystallographic data are summarized in Table IV. All data processing was performed on a Digital Equipment Corp. MICROVAX II computer by using the TEXSAN structure-solving *system obtained from the Rigaku Corp.*, Tokyo, *Japan. In data* reduction, Lorentz and polarization corrections were made. Block-diagonal matrix least-squares refinement[44,45] minimized the function $\sum w(|F_o| - |F_c|)^2$, where $w = 1/\sigma(F)^2$, $\sigma(F) = \sigma(F^2)/2F_o$, and $\sigma(F_o{}^2) = [\sigma(I_{raw})^2 + (0.02F_o{}^2)^2]^{1/2}/Lp$.

9c crystallized in a triclinic system. Intensity statistics indicated a centrosymmetric space group, and successful solution and refinement proved $P\bar{1}$ (No. 2) to be the correct choice. The structure was solved by a combination of direct methods (MITHRIL) and difference Fourier synthesis. All the non-hydrogen atoms were refined by using anisotropic thermal parameters. In the final least-squares cycles the hydrogen atoms attached to the Cp and Ph groups were fixed on the positions that were calculated by using idealized geometry and d(C–H) = 0.95 Å and were not refined [$B(H) = 1.2B(C)$]. The positions of the hydrogen atoms attached to the Fe atoms were confirmed by using isotropic thermal parameters.

Acknowledgment. This research was financially supported by a Grant-in-Aid from the Ministry of Education, Science, and Technology of the Japanese Government.

Supplementary Material Available: Tables of anisotropic thermal parameters and additional bond lengths and angles and numbering schemes for molecule 2 and the hydrogen atoms (12 pages); a table of calculated and observed structure factors (59 pages). Ordering information is given on any current masthead page.

---

(44) The positional and thermal parameters and the scale factor were blocked for each atom.

(45) As pointed out by one of reviewers, the rather large differences in the bond lengths and angles of the phenyl groups, ranging up to 14 esd's, may result from both the underestimated esd's from the block-matrix least-squares refinement and a substituent effect of Sn. For example, the averaged C–C lengths of **9c** are 1.380 Å (ipso–ortho), 1.385 Å (ortho–meta), and 1.361 Å (meta–para). A similar tendency has been observed for $CpFe(CO)_2{-}SnPh_3$[34] [1.39 Å (ipso–ortho), 1.44 Å (ortho–meta), 1.36 Å (meta–para)].